COMSOL
CONFERENCE
2023 MUNICH

Simulation of a hybrid (passive/active) acoustic measurement room

R. Boulandet[1], M. Allado[1], C. Pinhède[2], E. Friot[2], R. Côte[2], P. Herzog[3]
1. HEPIA, University of Applied Sciences and Arts Western Switzerland, Geneva, Switzerland.
2. LMA, Marseille, France.
3. ARTEAC-LAB, Marseille, France.

Abstract
The ideal way to measure the acoustic performance of heavy items such as vehicles or machines is in a semi-anechoic chamber, i.e. in an environment with no reflections except from the solid floor where the noise source is standing. To accurately measure low frequencies down to 20 Hz (lower limit of the audible frequency range), the walls and ceiling of the room should be non-reflective down to 20 Hz. This is a practical challenge as usual (passive) rooms involve absorbing material (wedges) on the anechoic walls, leading to a lower cut-off frequency related to the wedge thickness: the lower frequency limit corresponds to a thickness close to a quarter of the longest wavelength to be absorbed. For example, a typical wedge length of 0.9 m gives good measurements down to around 100 Hz. An anechoic chamber accurate to 20 Hz would therefore require more than 4 m thick wedges to provide adequate low-frequency absorption: such a test facility would be quite difficult to build and excessively expensive. An alternative has recently been proposed: the DADA (Dome Anti-Diffraction Acoustique). This hybrid control approach combines a thin layer of absorbent (passive) materials with an active system driving a set of loudspeakers designed to cancel out the low-frequency pressure field scattered by the walls. In this paper, we present the scattered field control strategy for room reflections and its implementation in a COMSOL Multiphysics model using the Pressure Acoustics, Frequency Domain interface and LiveLink™ for MATLAB® to run simulations. Results computed in a lightly damped rectangular room over a frequency range of 20 Hz to 200 Hz are provided to show the performance and limitations of the DADA solution in cancelling the scattered pressure field.

Keywords: semi-anechoic chamber, active control of scattered sound field, acoustic testing.

Introduction

An anechoic chamber is an experimental room whose walls absorb sound waves, reproducing free field conditions ideal for acoustic testing. It is the ideal place to characterize microphones and loudspeakers or low background noise emissions because the room does not cause reflections that could disrupt measurements. Basically, the acoustic energy emitted by the sound source under test is transmitted through the air in the form of pressure waves. As the waves travel through the absorbing material, they cause mechanical losses via the conversion of part of the sound energy into heat, resulting in acoustic attenuation. A wedge-shaped geometry further allows for a gradual change in the acoustic impedance of the transmission media, causing sound waves to be more effectively absorbed by the material. Current anechoic chambers typically provide accurate low-frequency acoustic measurements down to $70-100$ Hz depending on wedge length and material characteristics. Below this cut-off frequency, however, these rooms amplify sound excessively when subjected to dynamic excitation having a frequency close to one of its so-called natural frequencies [1, 2]. Measuring the sound level of a source would therefore be distorted at very low frequencies. This phenomenon of resonance is due to the presence of a constructive interference between incident and reflected waves. This creates standing waves, i.e. waves that bounce back and forth between the room walls and whose wavelength – or a multiple thereof – coincides with the room's dimensions. The alternative is to use active technology to minimize the pressure field scattered by the walls. The strategy is based on the principle that a unique linear operator maps the total acoustic field close to the walls to the field scattered by these walls, whatever the direct acoustic field [3] [4] [5]. This "scattering operator" can be first identified from off-line measurements involving a known direct pressure field and then used to calculate the scattered pressure field generated by an unknown direct field. A set of secondary sources distributed around the room is finally used to minimize this scattered sound field, as for an "ordinary" total sound field picked up by microphones.

In this paper, we present the implementation of a digital twin used to optimize the acoustic performance of such a hybrid measurement room by understanding its overall behavior, including its sensitivity to tuning and design parameters. We describe the modeling and calculation steps involved in cancelling the scattered pressure field, and present preliminary results showing the expected performance.

Modeling of the Measurement Room

This section presents the modeling of the active control strategy in a lightly damped room. **Figure 9** shows a view of the planned hybrid (passive/active) measurement room. A set of secondary sources (loudspeakers placed close to the walls) is controlled from the pressure field captured by an array of microphones (in red) delimiting a volume where we seek to minimize the contribution of the pressure field diffracted by the room. Additional microphones (in blue) are used to observe the effectiveness of the control in relation to the source to be characterized.

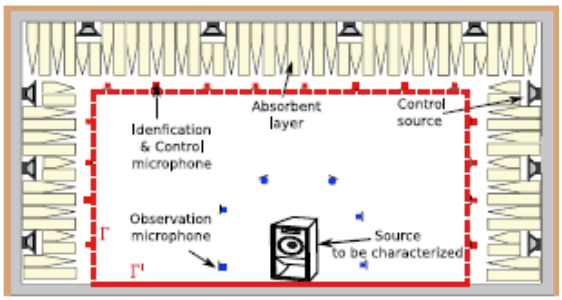

Figure 1. View of the planned hybrid (passive/active) acoustic measurement room.

Analytical modeling of a rectangular room

For a monopole point source and considering lightly absorbing walls, there is an analytical solution in three dimensions for the pressure at any point in the room. The pressure $p(\boldsymbol{r})$ can be expressed in terms of the Green's function $G(\boldsymbol{r}, \boldsymbol{r}_0)$, which is constructed from undamped room mode shapes evaluated at the receiver $\boldsymbol{r}$ and source $\boldsymbol{r}_0$ positions and a frequency-dependent damping term ξ_n. The expressions are:

$$p(r) = j\rho_0\omega q_0 G(\boldsymbol{r}, \boldsymbol{r}_0) \tag{1}$$

where ρ_0 is the density of air, ω is the driving angular frequency, and,

$$G(\boldsymbol{r}, \boldsymbol{r}_0) = \sum_n \frac{\psi_n^t(\boldsymbol{r})\psi_n(\boldsymbol{r}_0)}{(k_n^2 - k^2 + 2j\xi_n k_n k)\int_V \psi_n^2 \mathrm{d}V} \tag{2}$$

where ψ_n are the eigenfunctions representing the mode shapes as cosine functions, $f_n = ck_n/2\pi$ are the corresponding eigenfrequencies, and V is the room volume. The Green's function represents a triple summation over modes in the three orthogonal cartesian directions, with indices n representing the different modes. More details on the analytical description can be found in [2].

Scattered pressure field control strategy

Let $\boldsymbol{p}_{sca}$ be the pressure field scattered by the room at the minimization points when the primary source is operating alone. The vector $\boldsymbol{u}$ of control signals driving the secondary sources is determined by minimizing at each frequency:

$$J = \|\boldsymbol{p}_{sca} - \boldsymbol{C}\boldsymbol{u}\|^2 \tag{3}$$

where $\boldsymbol{C}$ is the system transfer matrix between the control sources and the resulting pressure at the minimization points. More details on analytical modelling can be found in [5].

Determining the scattered pressure field

In this section, we present the implementation of the control described above in a room as a two-stage process. The first step is to determine off-line all the transfer functions between the secondary sources located in the measurement zone and the minimization points distributed around it. **Figure 2** et **Figure 3** show the distribution of 72 monopole point sources and 62 minimization points allowing all transfer functions to be identified.

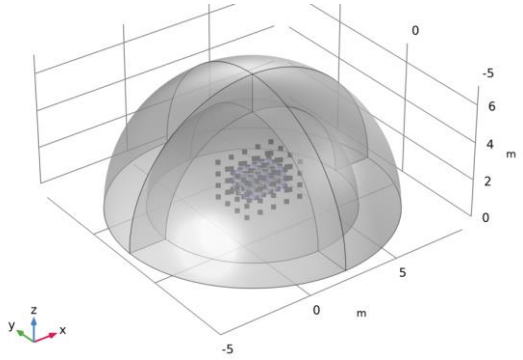

Figure 2. Geometry for the calculation of the direct pressure field where the 72 monopole point sources are regularly distributed in the blue box and the 62 minimization points are distributed all around.

An initial calculation is performed in a semi-open acoustic domain modeled by a sound hard boundary condition for the floor and ended by a perfectly matched layer (PML). Each of the monopole point sources shown in **Figure 2** is activated successively, providing a flow rate $q_0 = 10^{-4}$ m^3/s. This gives the direct pressure field $\boldsymbol{p}_{dir}$ at each of the minimization points distributed over a closed area surrounding the volume to be controlled (blue box).

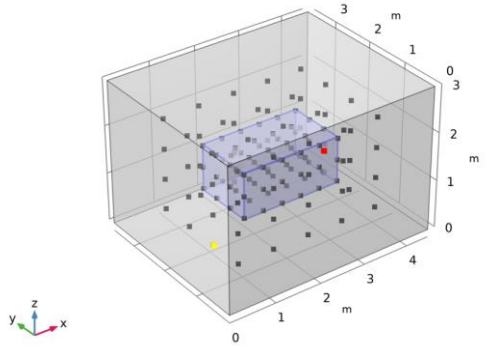

Figure 3. Geometry for the calculation of the total pressure field in the room where the 72 monopole point sources are distributed throughout the volume to be controlled (blue box) and the 62 minimization points are distributed all around.

Next, the total pressure field $\boldsymbol{p}_{tot}$ is calculated in the same way but considering now the rectangular

room, as shown in **Figure 3**. Then, the scattered pressure field in Eq. (3) is derived as

$$\boldsymbol{p}_{sca} = \boldsymbol{p}_{tot} - \boldsymbol{p}_{dir} \quad (4)$$

Successive activation of the sources and saving of results is done from a MATLAB code using LiveLink™ for MATLAB®.

Determining the system transfer matrix

The second step is to compute the system transfer matrix $\boldsymbol{C}$ in Eq. (*3*). The 54 secondary sources shown in **Figure 4** are activated one after the other as explained above. The normal acceleration is specified in the model as

$$a = j\omega q_0 / S \quad (5)$$

where $S = 0.0133$ m^2 is the area of the pistons. The resulting pressure field is evaluated at the 62 minimization points (see **Figure 4**), giving the transfer matrix $\boldsymbol{C}$ with dimensions $62 \times 54 \times 181$ over the frequency range 20 Hz to 200 Hz in steps of 1 Hz. The command $\boldsymbol{u}$ driving the 54 control sources is finally obtained by solving Eq. (3).

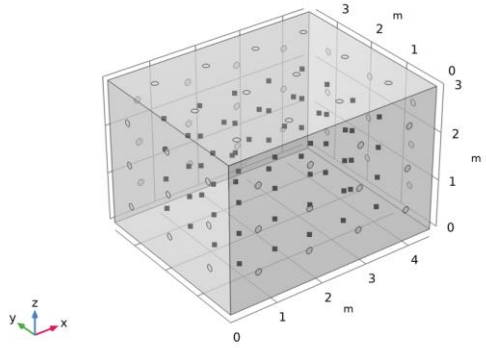

Figure 4. Geometry to determine the system transfer matrix where the 54 secondary sources are modeled as flush-mounted circular pistons and the 62 minimization points are distributed all around.

Simulation Results

Simulation parameters

In what follows, we consider a rectangular room measuring $4.5 \times 3.65 \times 3$ m^3. In the simulation, we used a constant specific acoustic impedance of $8 \cdot 10^4$ Pa.s/m for the walls (corresponding to an absorption coefficient of approximately 2% with a purely real impedance) and a sound hard boundary the floor. The flow rate imposed by the test source is 10^{-4} m^3/s. The simulations are run using the *Pressure Acoustics interface* available in the *Acoustics module*, in the frequency range 20 Hz to 200 Hz in steps of 1 Hz. The mesh is controlled by the physics of the model, considering the maximum wavelength of interest. The computation time required to solve the simulation, which includes 32'000 domain elements, is around 1500 s on a desktop computer for 181 frequency steps.

Room frequency response

The plot in **Figure 5** shows the results obtained for the direct response, the total response in the room with control on/off, and the contribution of the scattered pressure field. This is the frequency response between the monopole point source and the observation point indicated by red and yellow markers in **Figure 3**, respectively.

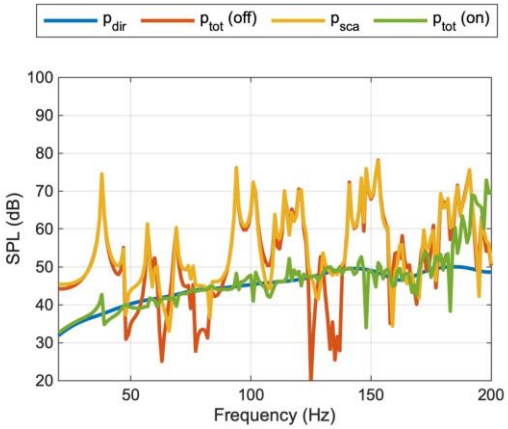

Figure 5. Room frequency response with control switched off/on

As can be seen in **Figure 5**, the room modal response with control off shows peaks and dips corresponding to the pressure anti-nodes and pressure nodes at the observation point, respectively. Note that the total pressure field $\boldsymbol{p}_{tot\,(off)}$ is mainly due to the scattered pressure field $\boldsymbol{p}_{sca}$. With control on, on the other hand, the total pressure field $\boldsymbol{p}_{tot\,(on)}$ tends towards the direct pressure field response of a monopole point source which would be placed at the same distance from a sound hard floor. This significantly attenuates the pressure field scattered by the room. However, this is no longer the case when the frequency exceeds around 180 Hz. This is linked to number of sources and microphones, whose spacing becomes greater than the wavelength.

Total pressure field with control off

The plot in **Figure 6** shows the pressure distribution in the room with control off at three different frequencies. These correspond to the first mode in the *x*– and *y*-directions and the first tangential mode in the *xz*–plan, respectively, and align well with the 1st, 2nd and 5th peaks on the plot in **Figure 5**. Pressure antinodes are shown in red and pressure nodes in blue/green. Although the calculated frequency step is relatively coarse, we find the expected modal shapes for room modes (100), (010) and (101), respectively.

Total pressure field with control on

The graphs shown in **Figure 7** illustrate the pressure distribution when the control is switched on.

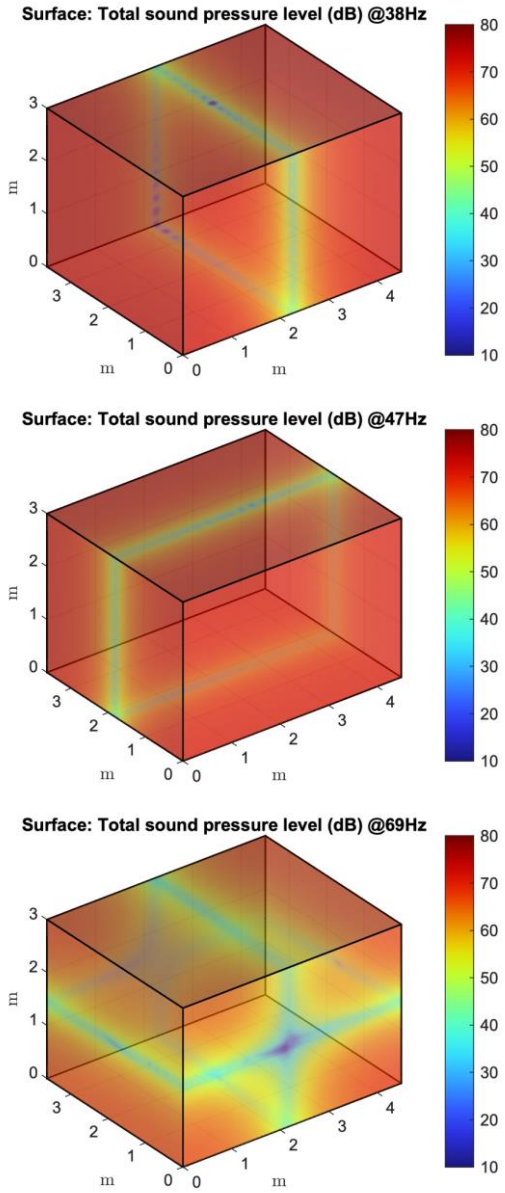

Figure 6. Total sound pressure level with the control off at 38 Hz, 47 Hz and 69 Hz.

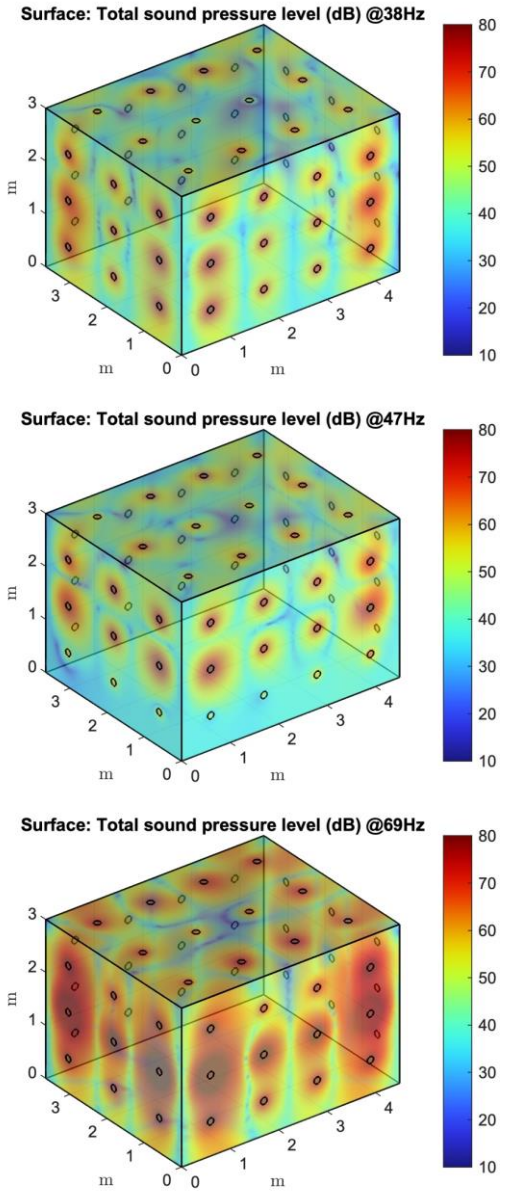

Figure 7. Total sound pressure level with the control on at 38 Hz, 47 Hz and 69 Hz.

It can be seen that the pressure distribution in the room no longer follows the structure of the uncontrolled room modes (**Figure 6**).
We can no longer distinguish either the pressure nodes or antinodes. On the other hand, we can see how the secondary sources work to minimize the pressure field diffracted by the room as a function of their positions relative to the test source.

Figure 8 shows the cross-sectional surfaces in the *yz*- plane of the test source, the position of which is indicated by a red spot near the center of the slice. As can be seen in **Figure 8**, the total sound pressure tends towards the free field response of the test source in a large volume around it. Near walls, on the other hand, higher sound pressure levels are due to the radiation of secondary sources to minimize the scattered pressure field. The results also show how the control effort applied to the secondary sources depends on the shape of the room modes to be controlled.

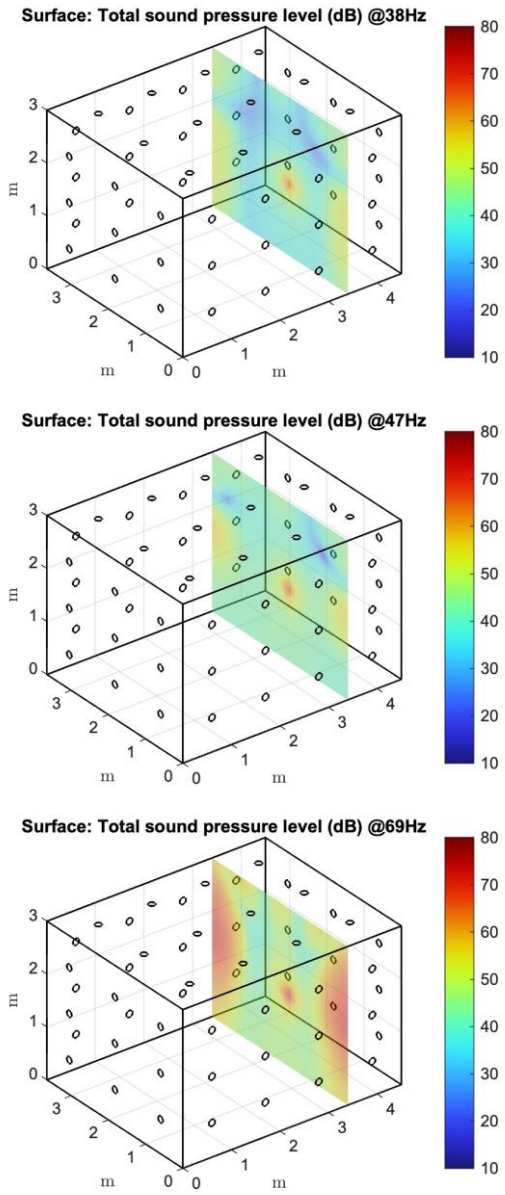

Figure 8. Slice plot showing how pressure is distributed inside the room with control the on at 38 Hz, 47 Hz and 69 Hz, in the yz-plane of the test source.

Characterization of the demo room

In what follows, we present results obtained in the demo room currently under construction at LMA (see **Figure 9**). The room is rectangular and 5.33×4.22×2.73 m3 in size. The walls and ceiling are made of double layered plasterboard (2×13 mm) and the floor is painted concrete. The access door is made of solid wood and the frame is fitted with seals. As can be seen in **Figure 9**, the loudspeakers and microphones of the active control system are positioned using a truss structure, which is also intended to support the panels of absorbent materials.

Figure 9. Photo of the actual demonstrator currently under construction at LMA.

Excitation is provided by a test source consisting of two push-pull loudspeakers (not shown in **Figure 9**) placed on the floor in one corner, with the measurement microphone in the opposite corner. **Figure 10** shows the frequency response of the source flow rate measured in the room shown in **Figure 9**, defined using an interpolation function in the model. More details on the sound source can be found in [6].

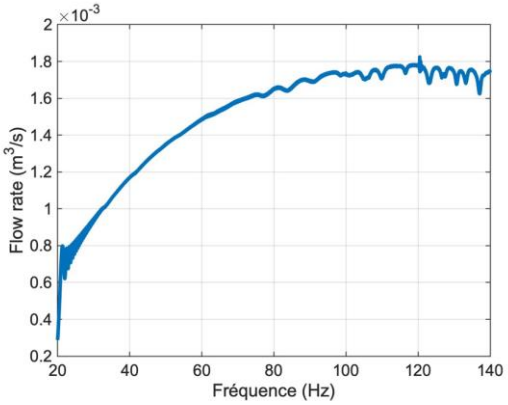

Figure 10. Measured frequency response function of the sound source output.

Figure 11 shows the computed frequency response in a corner of the room in terms of sound pressure level (SPL), compared with experimental measurement in the demo room described above. In the model, the wall impedance is specified using a frequency-dependent absorption coefficient obtained from measurements in the room shown in **Figure 9.** Furthermore, excitation is applied using a dual monopole point source whose output depends on frequency and is derived from measurements taken in the real room. Simulation is performed over the frequency range 20 Hz to 140 Hz, in steps of 0.125 Hz.

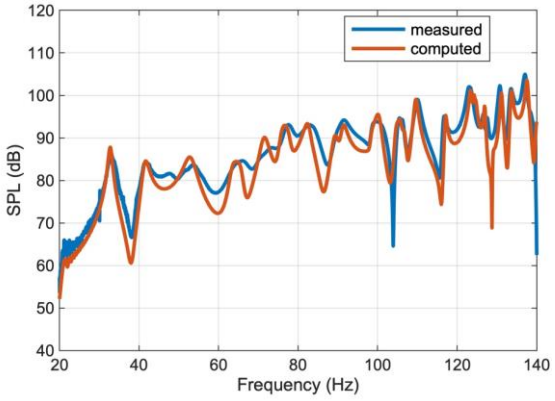

Figure 11. Frequency response function of the acoustic measurement room (with the active system switched off and without absorbing materials).

As can be seen from **Figure 11**, there is a good agreement between the experimental and numerical results. As expected, the room modes are far enough apart that the bandwidths of the modes do not overlap. The room modes are more damped compared with the response shown in **Figure 5**, which considers walls with lower damping. The discrepancies between measured and calculated data can partly be attributed to the presence of elements not considered in the model (truss structure for example), as well as to approximations in the positioning of the measurement and excitation points. These preliminary numerical results, recalibrated from experimental data, provide a more accurate picture of the actual response of an actively controlled room.

Conclusion

In this paper, we present the implementation of a digital twin of a hybrid (passive/active) acoustic measurement room. The approach of combining a COMSOL Multiphysics model using the Pressure Acoustics, Frequency Domain interface and LiveLink™ for MATLAB® to run simulations is proving effective in obtaining relevant results, partly derived from recalibration from experimental data. This gives us the room eigenmodes, adjusted for frequency and damping. To do this, we used the data measured in the real room under construction to adjust the wall impedance conditions and the flow rate of the test source in the model. This preliminary step provides a solid basis for studying the control strategy in a relatively well-controlled environment. For example, it becomes possible to study the influence of the placement and directional characteristics of the test source or the number and arrangement of secondary sources on the overall performance of the active control. The model allows, among other things, to study the effect of a regular or irregular distribution of secondary sources and/or minimization points, to avoid problems of singularities in the control matrices. Having the digital twin of the actively controlled room makes it possible to understand its overall behavior, including its sensitivity to tuning and design parameters. This allows control configurations to be quickly tested before considering their practical implementation in the real room. The next steps will be to include in the model the layer of absorbing material around the perimeter of the room (walls and ceiling) and to replace the simple piston geometry by a more realistic loudspeaker driver using a lumped model represented by an Electric Circuit physics. This would also make it possible to assess the power consumption required by the active control system with a view to optimizing it. This information provides a useful resource for improving the design and tuning parameters of tomorrow's active anechoic chamber, and therefore the technology they help to power.

References

[1] H. Kuttruff, Room acoustics (6th ed.), CRC Press, 2016.

[2] P. Morse and K. U. Ingard, Theoretical acoustics, Princeton University Press, 1986.

[3] C. Pinhède, D. Habault, E. Friot and P. Herzog, "Active control of the field scattered by the rigid wall of a semi-anechoic room—Simulations and full-scale off-line experiment," *Journal of Sound and Vibration*, vol. 506, pp. 116-134, 2021.

[4] D. Habault, E. Friot, P. Herzog and C. Pinhède, "Active control in an anechoic room : Theory and first simulations," *Acta Acustica united with Acustica*, vol. 103, pp. 369-378, 2017.

[5] C. Pinhède, M. Allado, R. Boulandet, R. Cote, E. Friot and P. Herzog, "Towards an active semi-anechoic room: simulations and first measurements," in *Forum Acusticum*, Turin, Italy, 2023.

[6] C. Pinhède and P. Herzog, "Design and measurement of a reference source at lower frequencies," e-Forum Acusticum, Lyon, France, 2020.

[7] E. Friot, R. Guillermin and M. Winninger, "Active control of scattered acoustic radiation: a real-time implementation for a three-dimensional object," *Acta Acustica united with Acustica*, pp. 278-288, 2006.

Acknowledgements

This work was supported as part of the France 2030 investment plan and the Aix-Marseille Université - A*MIDEX Excellence Initiative (AMX-19-IET-010).